

An iterative map analysis of heart rate variability in the neighborhood of stress induced chaos

Theophilus A. Fashanu, Olagoke K. Ale, Ayo Oyediran, and Viyon Dansu

Abstract—This work examines the viability of one-dimensional Poincare section as an iterative tool for the inversion of electrocardiogram obtained from stressed cardiovascular system. The response of Heart Rate Variability to induced stress in a healthy subject on a Modified Bruce Treadmill Protocol was processed to derive R-peaks in six batches of 5.06 minutes per batch. For each stage, a corresponding iterative map was constructed with the sequenced R-peaks using the Kubios software. With increasing intensity of induced stress, the maps outline the nonlinear dynamic response of the subject's autonomous nervous system. At the combined warm up stages one and two of the protocol, 1.6% offshoot in ANS activities is indicated with higher rate of parasympathetic activities. Response to low intensity stress condition showed symmetric ANS activities. However, with high intensity stress at the fifth stage, the map indicated an exponential increase in the number of heart beat orbits. However, the increment is characterized by skewed ANS activities with 15% acceleration of sympathetic ANS and 5% deceleration of parasympathetic activities. This profile is preserved at the final stage. In effect, the topology of the iterative maps of stages five and six of the protocol shows an inner ANS dynamical structure that is characterized by positive Lyapunov exponent. This limiting dynamical response determines the cardio-pulmonary reserve of the subject. Thus, Poincare iterative maps provide high resolution computational tool for identifying the onset of chaotic motion in stressed cardiovascular systems.

Keywords—Cardio-pulmonary Reserve, Heart Rate Variability, Iterative Maps, Nonlinear Dynamics.

I. INTRODUCTION

Cardiac disorder is a leading cause of mortality in humans [1]. In 2016, the World Health Organization (WHO) reported that cardiac disorder is responsible for almost one third of all deaths. Given that early detection of some asymptomatic non communicable medical conditions may improve cure and survival rates [2], science is continually developing innovative and high precision for early diagnosis of cardiovascular disorder and similar medical disorders.

Akinfenwa T. Fashanu is with the Department of Systems Engineering, Faculty of Engineering, University of Lagos, Yaba, Lagos, Nigeria. (Email: tfashanu@unilag.edu.ng, phone: +2348023263627).

Olagoke K. Ale is with the Cardiology Unit of the Department of Medicine, College of Medicine, Idiaraba, Lagos, Nigeria.

Ayowole Oyediran is with the Department of Mechanical Engineering, Faculty of Engineering, University of Lagos, Yaba, Lagos, Nigeria.

Viyon Dansu is with the Department of Systems Engineering, Faculty of Engineering, University of Lagos, Yaba, Lagos, Nigeria

In this regard, advances in computational and statistical methods are also making very important contributions toward accurate and timely diagnosis of some medical conditions.

They provide reliable qualitative and quantitative analyses of signals acquired from cardiovascular functions to enhance prognosis in ways that reduce missed diagnoses, and minimize time taken to reach accurate decisions. In effect, there is continuous reduction of morbidity and mortality resulting from cardiovascular disorder.

Developments in applied numerical analysis, soft computing and statistical techniques now provide additional support for early identification of patients' specific cardiac defect(s). In effect, a class of statistical discriminant functions are available for effective identification of some these medical disorderliness. However, given the inherent nonlinearity of the dynamics of cardiovascular system, the screening ability of traditional risk assessment tools is often challenged especially when some intricate clinical episodes are presented [3]. To address this issue, some analytical techniques that are developed for nonlinear dynamical systems have been used to diagnose the time response of cardiovascular systems [4]. In particular, [5] analyzed steady state response of the variability of cardiac pulse rate using the Poincare map. However, due to the intrinsic aperiodic nature of heart rate variability, this work investigates the potential of using Poincare map to identify the onset of nonlinear non-equilibrium period doubling dynamics i.e. chaos in a stressed cardiovascular system. This is achieved through an analysis of heartbeats response and their rates of variation. Given that cardiovascular stress can be induced by physical and pathological conditions, the viability of Poincare map to identify the onset of chaos under the prevalent condition would provide a reliable and proactive computational tool for monitoring the precipitation of crisis in stressed cardiovascular systems.

Heart rate variability (HRV) analysis is an established metric for assessing autonomic nervous system (ANS) functioning in cardiovascular research and related human wellbeing systems. HRV is a result of ANS modulation of the sinoatrial (SA) node. The sympathetic and parasympathetic units are ANS subsystems with significant influence on heart rate and its variability [6]. The sympathetic activity is known to increase heart rate and decrease rate variability. On the other hand, parasympathetic activity acts to decrease heart rate and increase its variability. On the whole, HRV can be a measure of cardiovascular stress and fitness, as well as a measure of other related pathological variables, [7].

Conceptually, the Poincare map is a numerical integration approach for visualizing the inner evolutionary structures of

dynamical systems. It gives a visual analogue of the exact nonlinear dynamics because the topology of its phase space describes the systems behavior in the neighborhood of prevalent fixed point(s). As a rule, topology of the phase space (of some iterative maps e.g. the Poincare plot) is a basis for determining the stability properties of system's fixed points and vice versa. Thus, iterative maps have found very useful applications in many fields including astrophysics, economics, engineering, geophysics, mathematics etc. Although, its reliability is often challenged in large dynamical systems due to the use of relatively long time intervals. In medical science, the Poincare map is gradually becoming a handy marker for heart rate variability analyses [8]. It is a more efficient operational tool compared with averaging method that is often considered alternative.

The averaging method for visualizing autonomous dynamical systems is semi-analytical. In principle, it is a perturbation analysis of complex dynamical systems presenting trajectories identical to those of linear systems. In its simplest form, the technique is a power series expansion that is truncated at certain admissible order. In some cases, the truncation error masks the underlying physics of the dynamical system. On the other hand, if many (i.e. higher) order terms of the approximating function are retained, the asymptotic perturbation series may not converge. This trend is common with the averaging approach since most of the nonlinear dynamical systems have no (or non-unique) integrands. Thus, the validity of the averaging method is limited to the neighborhood of stable and well-posed fixed points. Clearly, when a system develops chaotic motion with large perturbation from asymptotically stable equilibrium, the method of averaging fails. This structural behavior is typical of stressed cardiovascular system; hence the choice of the iterative Poincare map for visualization and analysis of heart rate variability in this work.

II. ADVANCES IN CLINICAL APPLICATIONS OF ITERATIVE MAPS OF HEART RATE VARIABILITY

In a pioneer work on the application of iterative maps for the visualization of heart beat dynamics, Przemyslaw *et al.*, [9] investigated the symmetrical properties of the heart rate R-R intervals in adults with normal cardiovascular functions. For this purpose, analytics of the Poincare plots were extended to define sub descriptors that describe heart rate symmetry. Five minutes ECG recordings of fifty healthy subjects were sampled. The first standard deviation from the line of identity i.e. SD1 was divided into two components, SD1_{up} and SD1_{down}. These describe the outcome of SD1 above and below the identity line of the Poincare plot of R-R intervals. Subsequently, binomial test was used to determine whether the probability of SD1_{up} > SD1_{down} is higher than the probability of SD1_{up} ≤ SD1_{down}. On the whole, the work established that probability marker for the upper rank R-R distribution from the identity line was significantly (i.e. 12%) higher than that of the lower rank. This revealed that the pattern of R-R interval changes differently during acceleration and deceleration of heart rate. Summarily, it was concluded that heart rate

acceleration (i.e. reduction of consecutive R-R intervals) and deceleration (i.e. widening of successive R-R intervals) are asymmetric.

In a related work, the effect of missing R-R-interval data on nonlinear heart rate variability analysis for a clinically impaired patient was studied, [10]. Simulated missing data in the actual R-R interval tachogram and actual missing R-R interval data was used for the analysis. Randomly selected R-R intervals ranging from one to a hundred samples were removed from actual data obtained from the MIT-BIH normal sinus rhythm R-R interval database. After a hundred Monte Carlo runs and Poincare sections of detrended fluctuation, and entropy of nonlinear HRV parameters in each run, authors concluded that nonlinear system identification processes that exclude the analysis of iterative Poincare maps may be inappropriate for accurate heart rate variability analysis especially if incomplete dynamical information is known.

Poincare analysis of heart rate variability has been used to explain cardiovascular autonomic function in obesity, [11]. The effect of obesity on cardiovascular activities using an iterative map was evaluated. It compared HRV of thirty-one obese adult males with body mass index BMI 26.84±2.47 of ages 25.42±2.86years with thirty-one normal male subjects of ages 25.38±4.61years. The map showed that decrease in parasympathetic activity in obese candidates' results in decreased heart rate variations. Scatter plots on the maps are concentrated towards the line of identity compared with those of normal subjects where the points are relatively divergent from the line of identity. Hence, the work established that heart rate variability is an effective index of the effect of obesity on cardiovascular autonomic function. Similarly, [12], analyzed the response of HRV to Cholinesterase inhibitor poisoning in humans.

III. THEORETICAL BACKGROUND OF THE POINCARÉ MAP

According to [13], the Henri Poincare map is an innovative tool for analyzing complex cyclic dynamical systems. Considering an autonomous rate system with periodic or quasi-periodic dynamics as represented by:

$$\dot{x} = f(x), \quad x \in \mathbb{R}^n. \quad (1)$$

Depending on the nature of $f(x)$, (1) may present periodic or quasi-periodic solution. Let $\mu(x, t)$, be a solution of (1) satisfying $\mu(x, 0) = x$. Then $O(x) = [\mu(x, t): t \in \mathbb{R}]$ is its orbit or trajectory passing through the point x .

Iteratively, an orbit of (1) can be approximated in small time increments. Given an initial value (x^0, t^0) , some numerical techniques may approximate the solution at successive grid points (x^k, t^k) , $k \geq 1$, such that the condition $x^{(k)} \sim \mu(x^0, t^k)$ is satisfied to construct a first return map. Thus, successive intersections of the trajectory are mapped on a co-dimension one surface of the phase space \mathbb{R}^n .

In this wise, the discrete phase variables x^k is plotted against discrete time values t^k to obtain an iterative transient approximation of the graph of $\mu(x, t)$. For the avoidance of doubt, this map differs from the phase portrait which is the plot of a phase variable with respect to another on the phase

plane.

For the autonomous system in (1), the existence of a Poincare map is far from obvious, and in many cases the map the trajectory, then there exists a positive and finite period T of the orbit, such that $\mu(x^0, T + t) = \mu(x^0, t)$ for all $t \in \mathbb{R}$. Specifically, $\mu(x^0, T) = \mu(x^0, t^0) = x^0$, so that the point x^0 returns to itself after it has flowed for period T .

Considering a surface ε that is transversal to the flow, i.e. the surface normal at $x^{(0)}$ satisfying $\langle n \in (x^{(0)}, f(x^{(0)})) \rangle \neq 0$; where $\langle \cdot \rangle$ denotes the inner product operator. By the implicit function theorem, an open neighborhood U of $x^{(0)}$ can be defined such that for all $x \in U$, there exists a positive number $\tau(x)$ such that if $z = \mu(x, \tau(x))$, then the following conditions apply:

(a) $z \in \varepsilon$ (x returns to the plane at point ε after time $\tau(x)$);
 (b) $\text{sign} \langle n \in (x), f(x) \rangle = \text{sign} \langle n \in (z), f(z) \rangle$ given that ε is approached from the same direction. The function $\tau : \mathbb{R}^n \rightarrow \mathbb{R}_+$ is continuous, and represents the time it takes for point x to return to ε according to condition (b). The point $z = \mu(x, \tau(x))$, is called the first return of x , and the Poincare map $P : U \rightarrow \varepsilon$ is defined by $P(x) = \mu(x, \tau(x))$. Clearly, by this definition, we have $\tau(x^{(0)}) = T$ and $P(x^{(0)}) = x^{(0)}$, [14]. These attributes supports iterative Poincare visualization of large time behavior of periodic/aperiodic nonlinear systems.

A. Acquisition and Pre-Processing of Stress Electrocardiograph Data

Stress ECG data for this study is obtained from a 175cm tall, 71.5kg, healthy, non-smoking, forty years old male adult. His body surface area is 1.94m^2 . Clinical history and physical examination of the subject yielded normal findings. He had normal resting electrocardiogram and normal haemogram. Modified Bruce thread- mill protocol was used to acquire stress ECG data. For the purpose of this work, the subject was marginally stressed beyond threshold 85% of predicted MCR heart rate. Details of the applied protocol is reported on Table I.

An in-house built data acquisition device was connected to ECG Lead I of the GE MAC 1200 monitor at D-3 Cardiograph, Surulere-Lagos, Nigeria. The acquired QRS complex is digitized at 500Hz with 12-bit resolution over $\pm 10\text{mV}$ range. Recording was done for a period of 36minutes. Also recorded are ten annotated beats (unaudited R-waves and T-waves peaks annotations from an automated detector).

In addition to the QRS complex, P and T waves, the waveform also contains 60-Hz noise from power line interference. This is in addition to convolution noise from electromyogram (EMG) due to muscles motion, artifacts from electrodes-skin interactions, as well as interference from other hardware in the surrounding. Consequently, the QRS complex is extracted the by a band pass filter.

B. Preprocessing of Acquired Stress ECG Data

R-peaks detection is fundamental in electrocardiogram data analysis. Given that Poincare method examines heart rate

may not exist. However, the iterative map is defined if the system admits periodic or aperiodic solutions. As a result, if x^0 is a point on variability through the inter-beat interval, it is important to obtain accurate values of R-R interval from ECG data. However, the challenges include; irregular distance between ECG peaks, irregular peak form, presence of low-frequency component in ECG due to subject respiration. Hence, the pre-processing algorithm is designed to minimize noise. At this stage, low frequency components are removed from raw ECG signal. Subsequently, the signal is processed in frequency domain through the use of Fast Fourier Transform (FFT). This enables the removal of convoluted noise. Subsequently, the Inverse Fast Fourier Transform (IFFT) returns the ECG signal to time domain. This is followed by the detection of R-peaks through the use of windowed filter to find local maxima. Finally, an optimum threshold is defined such that the preprocessing algorithm uses relative differences to register only significant values of R-peak.

C. Construction of Poincare Map using Preprocessed ECG Data.

To visualize the dynamics of the inter-beat intervals (i.e. the R-R intervals) on an iterative map, the detected R-peaks are sequenced as $R_1, R_2 \dots R_{n-1}, R_n$. The sequence is then regrouped into piece-wise pairs $(R_1, R_2), (R_2, R_3) \dots (R_{n-1}, R_n)$. Following [14], consecutive nodes were connected to track the trajectory of the inter-beat intervals. The value of n at each stage of the analysis is determined by the number of detected R-peaks. Clearly, given the cyclic nature of heart beats, these R-peaks are linearly independent. Precisely, the $(n-1)$ hyperplane C is constructed by specifying a point x_C on the plane and constructing its normal direction field $h = f(x_C)$. Using the method of [15], positions of the limit cycles are identified as $x_C = x^*$. Thus, identically, x^* is a fixed point of $f(x_C)$. Therefore, Poincare plot of HRV is a scatter plot of the current R-R interval plotted against the preceding R-R interval. Points above the line of identity indicate R-R intervals that are longer than the preceding R-R interval, and points below the line of identity indicate a shorter R-R than the previous. In line with the requirements of the sequence of R-peaks for the construction of the Poincare map.

D. Poincare Maps and Identification of Chaotic Dynamics

In context, chaos is aperiodic long-term behavior of deterministic systems that exhibit sensitive dependence on initial conditions. Aperiodic long-term behavior implies the onset of trajectories that do not settle down to fixed points, periodic orbits, or quasiperiodic orbits as time tends to infinity. Here, deterministic system is described as one with no random/noisy inputs or parameters. Also, system's irregular behavior is due to nonlinearity and not from noisy excitations. Finally, sensitive dependence on initial conditions indicates that orbits originating from a close neighborhood separate exponentially fast. According to [16], this response implies

that the system has a positive Lyapunov exponent in the neighborhood of the prevalent fixed point.

Table I. Modified Bruce Stress Thread-Mill Procedure

Stage	Speed km/h	Grade %	METS	Time Progression (min)		Analysis Duration (min)	Heart Rate (bpm)	
				Start Time	Stop Time		Initial	Final
1.	1.1	0.0	1.0	0.03	1.38	1.35	68	77
2.	1.6	0.0	1.2	2.20	3.02	1.18	77	83
3.	2.7	10.0	4.6	3.48	7.41	3.53	83	99
4.	4.0	12.0	7.0	8.21	14.11	5.50	99	108
5.	5.4	14.0	10.0	15.53	24.43	8.50	108	120
6.	6.8	16.0	12.5	25.27	30.36	5.09	120	151
7	6.8	16.0	12.25	30.41	35.53	5.12	151	169

E. Ellipse Fitting for Topology Analysis

To identify onset of chaotic dynamics in the stressed cardiovascular system, ellipse is inserted on the map for topology. In concept, ellipse facilitates analyses of the type one genus iterative map. To insert the ellipse, centroid of all the R-R interval data points is determined to locate the coordinate of its center. Subsequently, the vector of the relative position of each point with respect to the center is constructed and pre-multiplied by its transpose to obtain a 2×2 matrix. The resulting matrices are summed to obtain a single 2×2 matrix. Finally, direction and length of the ellipse axes are determined by the Eigen-vector and Eigen-values of the realized matrix.

Basically, the larger eigenvector determines the magnitude and direction (i.e. SD2) of the maximum variance of the R-peak distribution. On the other hand, the smaller orthogonal eigenvector shows the magnitude and direction (i.e. SD1) of its minimum variance. Thus, SD1 and SD2 are the minor and major axes of ellipse fitted on the map. These standard descriptors are quantitative measures for classifying the geometry of genus one type iterative map. In terms of linear statistics, these standard descriptors guide visual inspection of the R-R distribution for chaos identification. It reveals a useful

pattern of the R-R interval data by representing both short and long term variations of the signal. SD1 shows the standard deviation of the short-term variability of the data while SD2 shows standard deviation of the continuous long-term R-R intervals. The point where both axes intersect corresponds to the mean of the R-R intervals.

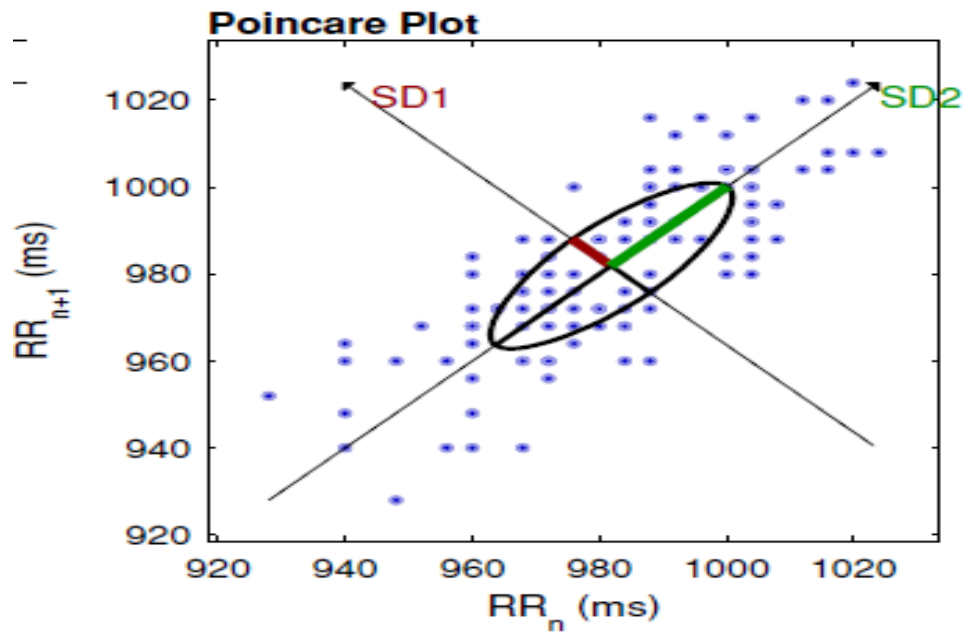
IV. RESULTS AND DISCUSSION

As stated in section 3.2, R-peak detection and noise removal are the fundamental electrocardiogram preprocessing operations for the Poincare plots. Standard algorithm for R-peak detection on the Kubios was repeatedly applied with the Fast Fourier transform for data processing and filter noise in frequency domain. The R-peak detection process is repeated for other samples and the corresponding Poincare Plots for each of the samples are presented in Figures 1 to 5. Data is acquired for a period of 30.36 minutes. For the objective of this study, the R-R intervals were grouped into five samples. The Poincare map and corresponding statistical measures were obtained in the manner of [17].

Statistical Markers	Samples 1 and 2	Sample 3	Sample 4	Sample 5	Sample 6
Mean R-R(ms)	976.2	984.9	985.7	1049.9	1049.6
Standard deviation R-R(ms)	19.2	46.9	43.4	161.13	161.10
Mean Heart Rate(/m)	61.13	62.18	60.99	58.526	58.541
Standard deviation Heart Rate(/m)	1.20	3.04	2.77	9.0980	9.0941
SD1(Standard deviation1)(ms)	8.7	10.7	11.0	38.584	34.526
SD2(Standard deviation2)(ms)	25.8	65.3	60.6	225.31	225.29

Table II. Statistical Attributes of Samples

Fig. 1: Poincare plot of the Sample 1 and 2



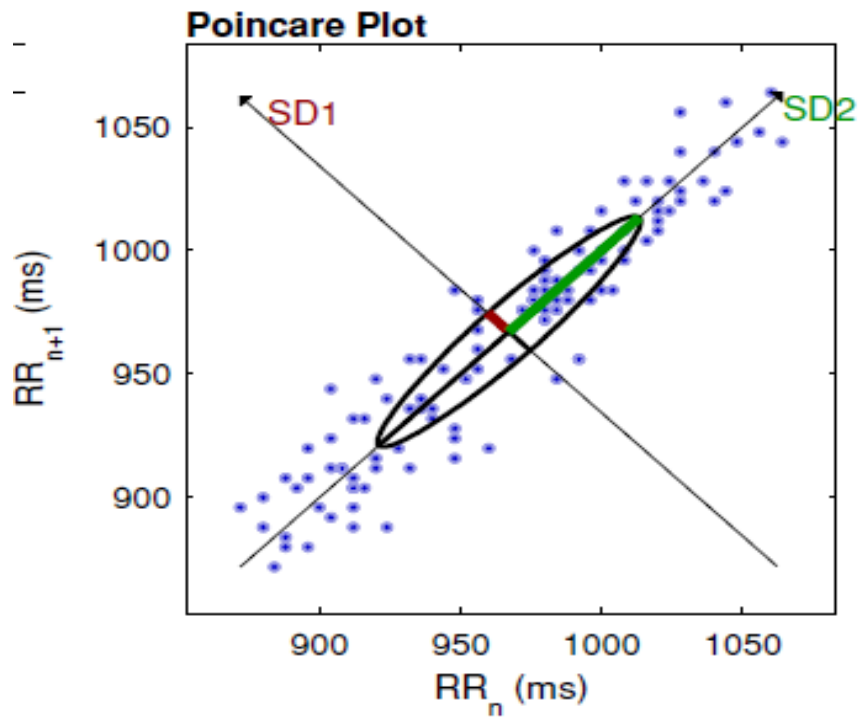


Fig. 2: Poincare plot of the Sample 3

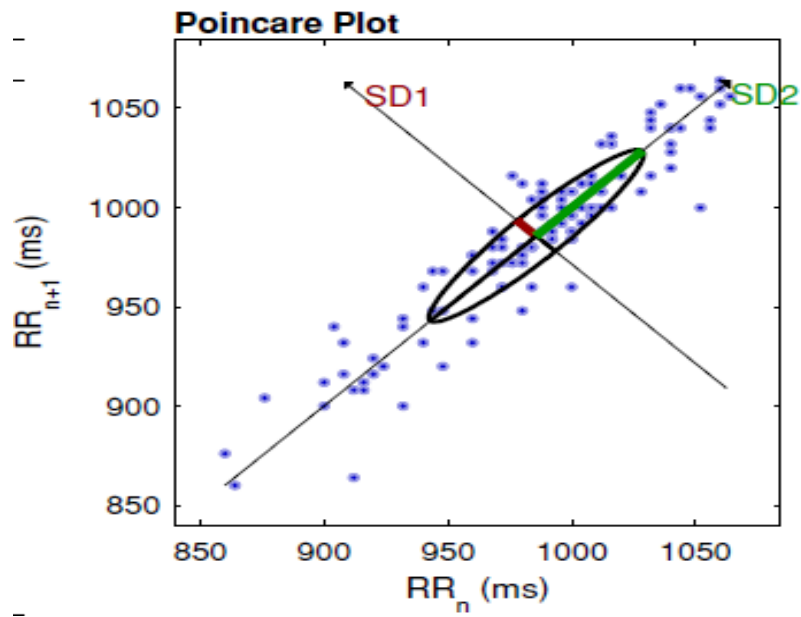


Fig. 3: Poincare plot of the Sample 4

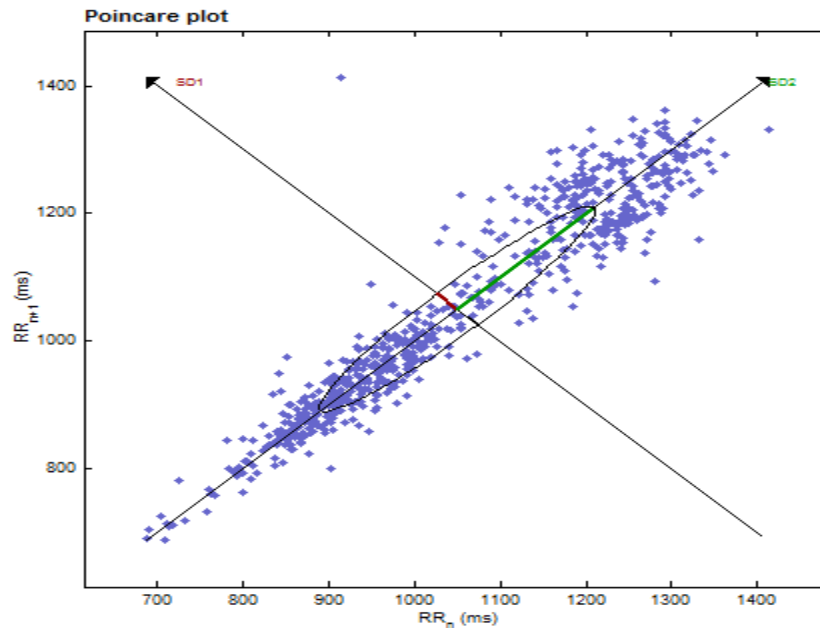
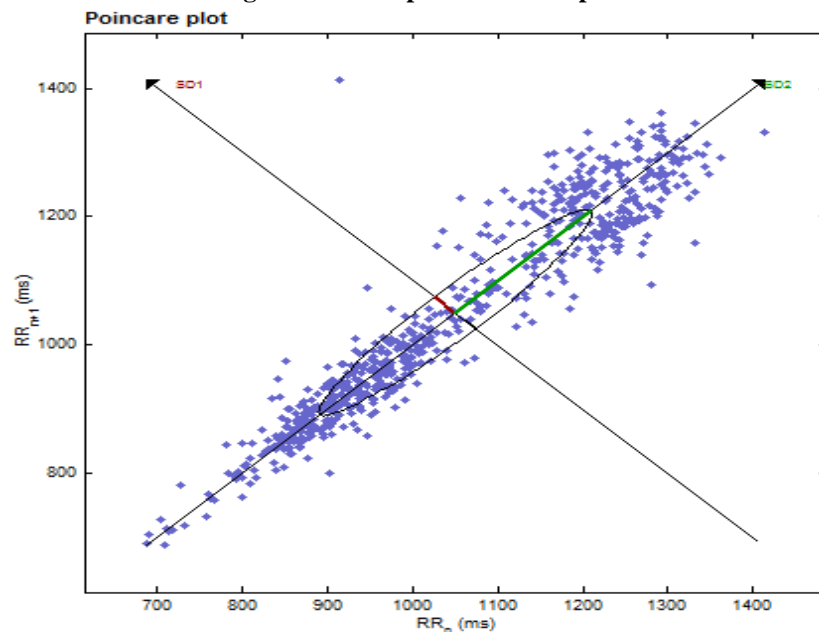


Fig. 4: Poincaré plot of the Sample 5

Fig. 5: Poincaré plot of the Sample 6



A. Discriminant Measures for Chaos Identification on Poincaré Maps

The topological layout of continuous interplay of sympathetic and parasympathetic response of the subject's autonomic nervous system resulting from stress variation and its effect on his cardiovascular condition are described in Figures 1 to 5. Precisely, the iterative map of the warm up state of the stress ECG test consisting of pre stress stages 1 and 2 is shown in Figure 1. The corresponding statistical attributes of detected R-R intervals at the warm up stages are detailed in Table II. On the iterative map, the inserted ellipse

illustrates that only 32.56% of sampled heartbeat dynamics has precise closed orbits with equal periods. The remainder are aperiodic and uniformly distributed outside the ellipse in the four quadrants outlined by the SD1 and SD2 axes at an average of 17.44% per quadrant except for the first quadrant with marginally fewer (i.e. 16.28%) orbits. This profile, implies a well behaved dynamics with near symmetry between sympathetic and parasympathetic activities except for 0.016 probability of parasympathetic activities exceeding sympathetic activities of the ANS.

At stage three of the protocol, the response of the subject's HRV is characterized by Poincaré section shown in Figure 2.

The detailed test conditions are specified on Table I, while the statistical attributes of acquired signal are summarized on Table II. Compared with stages 1 & 2; there is relative reduction of the numbers of closed orbits with equal period. This is indexed by increased eccentricity of inserted ellipse as shown in Figure 2. In this case, only 24.53% of the trajectories have a specific period. Also, the total number of non-unique aperiodic orbits have increased. Hence, the onset of a period doubling process is established. However, the process is skewed in favour of sympathetic activities. Collectively, the number of aperiodic orbits on the lower part of the SD2 axis is approximately 3.78% higher than orbits on the upper SD2 axis. Meanwhile, the lower and upper quadrants defined by the SD1 axis have equal number of aperiodic orbits. Thus, there is a steady increment in sympathetic ANS activities, and a delay in the response of corresponding restorative parasympathetic activities.

Next, the intensity of stress in the exercise is increased to stage four of the protocol. Corresponding test variables for this stage are also listed on Table I. The statistical attributes of the outcome of sampled signal are as reported in Table II. At this stress level, only 34.28% heart beats are completed in an exact period. The remainder are aperiodic orbits, located in the upper and lower parts of SD1/SD2 axes. In distribution, exactly 29.53% and 26.66% aperiodic beats are located outside the ellipse on the upper and lower bands of the SD2 axis. At the same time, 28.57% and 27.62% are orbits without specific periods. Though this structure is ergodic, it is apparent at this stage that parasympathetic activities are accelerating on both sides to resolve the stress induced heart rate acceleration by the sympathetic ANS of the subject. This distribution is delineated by the realization of a more eccentric ellipse on the Poincare section in Figure 3 when compared with Figure 2.

At the fifth stage of the test protocol; there is rapid increase in the total number of orbits as shown by the detected R-R intervals. This indicates a positive Lyapunov exponent in the underlying structure of the systems dynamics. In addition, the outline of inserted ellipse is further tapered, accommodating only 27.86% periodic orbits. On the upper and lower sides of the SD2 axis are 33.75% and 38.46% aperiodic orbits. On the other hand, aperiodic orbits on the upper and lower parts of the SD1 axis are 43.96% and 28.25% respectively. This structure revealed pronounced difference between sympathetic and parasympathetic ANS activities. Thus, according to Figure 4, sympathetic activities are significantly accelerated beyond the restorative response of parasympathetic activities. This realization indicates the precipitation of chaotic terminal order of HRV dynamics.

Furthermore, relative to the third stage of the protocol, the number of orbits indicated by the R-R interval at the penultimate and final stages have doubled. However, replicating exponential increment in number of orbits in autonomous cyclic systems is the benchmark index of fully developed chaotic motion. In topology, the map shows 30.91% periodic heart beats. Though there is an apparent increase in the fraction of periodic orbits when compared with

stage 4; the increment is transient and a realization of systems nonlinearity. Furthermore, Figure 5 shows a widened gap between the sympathetic and parasympathetic ANS activities as indexed by the distribution of aperiodic orbits. There, are 33.51% and 35.58% outliers across the upper and lower SD2 axis. This is against 41.20% and 27.89% aperiodic orbits flanking the upper and lower bands of the SD1 axis. Clearly, there is a limiting ability of the receding parasympathetic activity to regulate the randomly accelerating heart beats. This response suggests that the dynamics is limiting at this stage, and has attained the cardio-pulmonary reserve of the subject.

V. CONCLUSION

Cardiovascular disorder is a leading cause of morbidity and mortality across the globe. Hence, development and advancement of prognostic techniques for early and efficient detection of cardiac disorderliness would minimize consequent paralysis and untimely death. Thus, this work extends biomedical applications of one-dimensional Poincare sections to include computational inversion of electrocardiogram data. The developed iterative maps for ECG signals acquired from a subject on a Modified Bruce Treadmill protocol show significant sensitivity to stress level as well as sufficient ability to identify terminal dynamics of the cardiovascular system as the subject approaches the limit of cardio-pulmonary reserve. Hence, the Poincare map presents a high resolution numerical inversion scheme for assessing the impact of cardiovascular stressors at varied intensities using electrocardiogram data.

REFERENCES

- [1] World Health Organization, "Cardiovascular disease," 2016. [Online]. Available: http://www.who.int/cardiovascular_diseases/global-hearts/Global_hearts_initiative/en/.
- [2] M. Ntsekhe and A. Damasceno, "Recent advances in the epidemiology, outcome,," *Heart Online First*, 16 May 2013.
- [3] D. M. Stanley, C. Alkis and M. V. Prabhas, *Numerical Methods in Biomedical Engineering*, 2006.
- [4] E. G. Tolkacheva and F. X. Z. Brian, "Nonlinear and Computational Dynamics in Biomedical Applications," *Journal of Computational and Nonlinear Dynamics*, vol. XIII, no. 6, 2018.
- [5] Y. Chou, R. Zhang, Y. Feng, M. Lu, Z. Lu and B. Xu, "A Real-Time Analysis Method for Pulse Rate Variability Based on Improved Basic Scale Entropy," *Journal of Healthcare Engineering*, p. 10, 2017.
- [6] R. Metelka, "Heart rate variability - Current diagnosis of the cardiac autonomic neuropathy. A review,," 2014.
- [7] G. Berntson, D. Eckberg, P. Grossman, P. Kaufmann, M. Malik, H. Nagaraja, S. Porges, P. Saul, P. Stone and D. Molen M V, "Heart Rate Variability: Origins, Methods, And Interpretive Caveats," 1997, p. 623–648.
- [8] M. Brennan, M. Palaniswami and P. Kamen, "Trans. Biomed. Eng.," *IEEE*, 2001.
- [9] G. Przemyslaw, P. Jaroslaw and k. Tomasz, "Heart rate asymmetry by Poincare plots of R-R intervals. *Biomed Tech.*," pp. 272-275, 2006.
- [10] K. K. Ko, J. B. Hyun, G. L. Yong and S. P. Kwang, "Effect of missing R-R-interval data on nonlinear heart rate variability analysis. *Computer Methods and Programs in Biomedicine.*," pp. 210-218, 2012.
- [11] M. Krishnan, B. Kabali, J. M. Sajjadh and V. R. Badanidiyur, "Poincare Plot of Heart Rate Variability: An Approach towards Explaining the

Cardiovascular Autonomic Function in Obesity," *Indian Journal of Physiology and Pharmacology*, pp. 31-37, 2013.

- [12] K. Yongin and J. Jinwoo, "Heart rate variability analysis in acute poisoning by cholinesterase inhibitors," vol. 13, pp. 33-40, 2017.
- [13] R. S. Wayne, C. H. Kathleen, M. T. Xavier and G. Christoph, *Enhanced Visualization and Autonomous extraction of Poincare Map Topology*, 2013.
- [14] P. Jinho, L. Sangwook and J. Moongu, "Atrial fibrillation detection by heart rate variability in Poincare plot," *Biomedical Engineering Online.*, 2009.
- [15] S. P. Thomas and O. C. Leon, *A Textbook on Practical Numerical Algorithms for Chaotic Systems.*, 1989.
- [16] H. Stowgatz Steven, *Nonlinear Dynamics and Chaos.*, Perseus Books Publishing, L.L.C, 1994.
- [17] M. P. Tarvainen, J. P. Niskanen, J. A. Lipponen, P. O. Ranta-Aho and P. A. Karjalainen, *Kubios HRV-heart rate variability analysis software, Computer Methods and Programs in Biomedicine*, vol. 113, 2014, p. 210-220.
- [18] D. H. John, "The Poincare map and the method of averaging: A comparative study.," Thessaloniki, Greece.